

PAPER • OPEN ACCESS

Accelerated material development for laser powder-bed fusion using the arc melting process

To cite this article: M Reiersen *et al* 2023 *IOP Conf. Ser.: Mater. Sci. Eng.* **1274** 012014

View the [article online](#) for updates and enhancements.

You may also like

- [Laser-induced plume investigated by finite element modelling and scaling of particle entrainment in laser powder bed fusion](#)
Y A Mayi, M Dal, P Peyre et al.
- [Applications of artificial intelligence and machine learning in metal additive manufacturing](#)
Leila Jannesari Ladani
- [Improvement in the PBF-LB/M processing of the Al-Si-Cu-Mg composition through the use of pre-alloyed powder](#)
A Martucci, F Gobber, A Aversa et al.



ECS The Electrochemical Society
Advancing solid state & electrochemical science & technology

243rd Meeting with SOFC-XVIII

Boston, MA • May 28 – June 2, 2023

Accelerate scientific discovery!

[Learn More & Register](#)

Accelerated material development for laser powder-bed fusion using the arc melting process

M Reiersen^{1,3,*}, A E Gunnaes², A S Azar³, S Diplas³, Q Du³ and M. M'hamdi³

¹ *Department of Chemistry, University of Oslo, Oslo, Norway*

¹ *Department of Physics, University of Oslo, Oslo, Norway*

² *SINTEF Industry, Oslo, Norway*

* corresponding author: magnus.reiersen@sintef.no

Metal additive manufacturing has in recent years gained an increasing amount of attention, especially the subgroup of laser powder-bed fusion and aluminium alloys. However, established alloys are designed for casting and forging and often require alterations to make them eligible for the challenging processing conditions. The material selection is limited and calls for new alloys tailored specifically for additive manufacturing. In this work, an analysis suite is proposed as a tool to investigate material systems quickly and in-expensively for use in additive manufacturing. The selected material system is the Al7075 aluminium alloy, which is susceptible to cracking caused by hot tearing. To resolve this issue, it is mixed with varying quantities of silicon. The effect of silicon on solidification, grain refinement, and the resulting crack susceptibility is investigated with thermodynamical calculations considering the columnar to equiaxed transition, optical microscopy, and scanning electron microscopy after being processed by arc melting. The thermodynamical calculations of the compositions indicated a trend between the decreased columnar to equiaxed transition point at elevated temperature gradients to the silicon concentration. The experimental results reflected a similar trend by observing the reduction of the average grain size in the material system from 2470 μm^2 to 323 μm^2 for a composition with 0 wt.% and 10.5 wt.% silicon respectively. A composition of interest from the result was further mixed with zirconium hydride to investigate its grain refining properties on the alloy. The average grain size was reduced from 1055 μm^2 to 453 μm^2 by the inclusion of 0.24 wt.% zirconium. As such, this work provides a new approach to investigating a material system for use in additive manufacturing.

Keywords: Laser Powder-Bed Fusion; Selective Laser Melting; Additive Manufacturing; Arc Melting; Material Development; Material Screening

1. Introduction

Additive manufacturing has evolved rapidly in the past decade, whereas research is focused on plastic, ceramic, metallic and even organic components. AM technologies allow for the production of complex geometries in a layer-by-layer fashion, and the most widespread processing method for metal components is the Laser Powder-Bed fusion technique. Aluminium alloys are extensively used in various industries for their high specific strength, good corrosion resistance and low production cost [1], [2]. The starting point for aluminium alloys processed by Laser Powder-Bed fusion comes from well-established alloys, which have compositions specifically tailored for conventional casting and forging techniques. A material processed with Laser Powder-Bed fusion experiences rapid solidification in comparison to slow cooling in the conventional methods and therefore are compositions of established alloys not always directly transferrable to AM processing. The challenging environment limits the

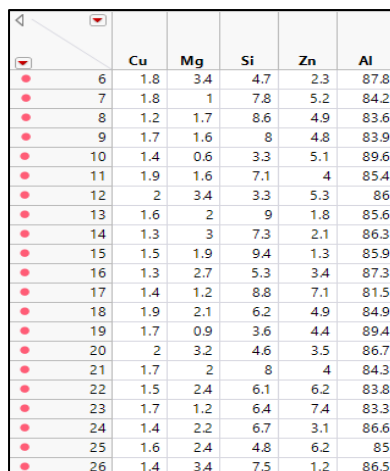


selection of available materials, and investigating a material system with the Laser Powder-Bed fusion process is expensive and time-consuming. Arc melting is proposed as a faster processing technique for the initial step of screening a larger amount of compositions in a potential material system to effectively find suitable candidates.

Aluminium alloys feature moderate material strength and ductility, and the goal is therefore to find other aluminium alloys with material strength comparable or superior to the wrought alloy. In the 7xxx series the Al7075 alloy is of interest due to its high specific material strength and a large area of application [3]. However, the established Al7075 alloy is highly susceptible to cracking when processed under rapid solidification conditions as present in Laser Powder-Bed Fusion, and the composition must therefore be altered to face these challenges. The main method to achieve this goal is by microalloying with other elements. So far silicon, scandium, zirconium, titanium and vanadium have proven as effective microalloying elements for aluminium alloys [[4], [5], [6], [7]]. Al7075 alloyed with silicon is the selected material system chosen for this work, whereas silicon is introduced to eliminate solidification cracking and in addition to acting as a grain refiner for the microstructure. Another method which is investigated in this work is the effect of adding nanoparticles of ZrH_2 to further refine the microstructure.

The present work aims to show that arc melting in combination with rapid analysis can be used as a method of rapidly screening potential material systems to find suitable candidates in an early stage of material development for additive manufacturing.

2. Experiments



	Cu	Mg	Si	Zn	Al
6	1.8	3.4	4.7	2.3	87.8
7	1.8	1	7.8	5.2	84.2
8	1.2	1.7	8.6	4.9	83.6
9	1.7	1.6	8	4.8	83.9
10	1.4	0.6	3.3	5.1	89.6
11	1.9	1.6	7.1	4	85.4
12	2	3.4	3.3	5.3	86
13	1.6	2	9	1.8	85.6
14	1.3	3	7.3	2.1	86.3
15	1.5	1.9	9.4	1.3	85.9
16	1.3	2.7	5.3	3.4	87.3
17	1.4	1.2	8.8	7.1	81.5
18	1.9	2.1	6.2	4.9	84.9
19	1.7	0.9	3.6	4.4	89.4
20	2	3.2	4.6	3.5	86.7
21	1.7	2	8	4	84.3
22	1.5	2.4	6.1	6.2	83.8
23	1.7	1.2	6.4	7.4	83.3
24	1.4	2.2	6.7	3.1	86.6
25	1.6	2.4	4.8	6.2	85
26	1.4	3.4	7.5	1.2	86.5

Figure 1. Composition matrix created by the design of experiments. Each element is randomly selected within a set range, creating compositions with a large variation of elemental combinations.

A design of experiments model is used to create a matrix of 65 compositions from elements in a set range close to the nominal composition of Al7075 with silicon included in a range of 0 to 10 wt. %. Some of the generated compositions are presented in figure 1. Columnar to equiaxed transition (CET) calculations are used on the different compositions to gain a better understanding of how the material system behaves during solidification, to study the effect each element has on the transition point at varied temperatures gradients. The thermodynamical model used is the Gaumann model, a modification of the Hunt model for CET calculations [8]. The result from these calculations is used to choose 10 compositions for further investigations in addition to two compositions with 0 wt. % and 0,4 wt.% silicon to cover the low silicon content region. For the experimental work, each composition is created by combining elemental powders, which are mixed and pressed into pellets. Arc melting the pellets melts the material into button-shaped metal pieces, which are thereafter cut, polished and lightly etched then investigated with optical and electron microscopy. An illustration of the arc melting process is presented in figure 2. In an attempt to further refine the microstructure, one of the compositions is mixed

with 0,5 wt.% and 0,8 wt.% zirconium hydride nanoparticles. The material is processed and investigated with the same procedure as described.

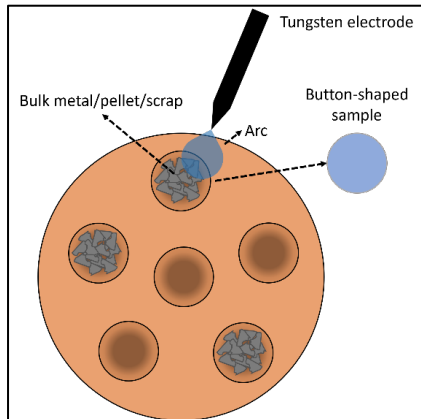


Figure 2. Arc melting setup. An electric arc from a tungsten electrode ionises an argon atmosphere and melts the material in a copper crucible mould. The arc is turned off and water circulation quickly cools the mould and material.

3. Analyses

3.1. Columnar to equiaxed transition calculations

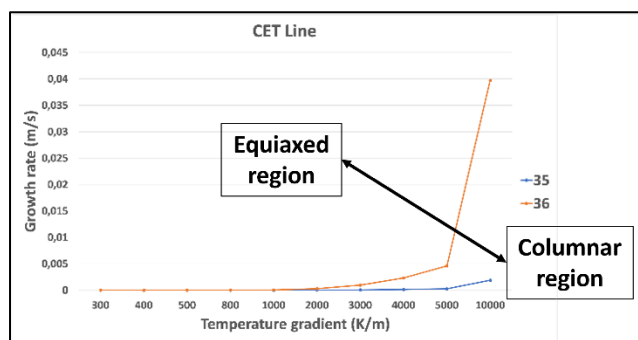


Figure 3. Columnar to equiaxed transition curve for two different compositions. At 10000 K/m the transition point for composition 35 is lower than 36, meaning a lower growth rate is required to be in the equiaxed region at higher temperature gradients. A decrease in the columnar to equiaxed transition point can increase the ratio of equiaxed to columnar grains or refine a fully equiaxed microstructure.

Alloy composition is the main variable when calculating the CET point. Varying certain elements will change the result from the model, where an example of which can be observed in figure 3 where two CET curves are plotted together. The graph shows the specific curve for two different compositions, where the main point of interest is on the y-axis at a point on the curve. For example, at a temperature gradient of 10^4 K/m on the x-axis, the value on the y-axis determines the critical growth rate for a transition between equiaxed and columnar dendritic grain growth. Varying the alloy composition shifts the transition point on the curve at a given temperature gradient, and this effect can be taken advantage of in investigations of new alloy systems. CET calculations can be used to investigate what and when the transition occurs, but in this work, the main purpose is to use it as a tool to predict what compositions favour the desirable equiaxed grain growth the most. In laser powder-bed fusion the growth rate and temperature gradients for a defined set of processing parameters can be calculated for a given composition. In real processing, there will be slight local variations in the growth rate and temperature gradients, but as an example let us assume it to be a fixed point. Under this assumption, the point can be placed in the graph observed in figure 3 containing two CET curves representing different compositions. The transition curve for composition 35 is significantly lower than composition 36 at higher temperature gradients, and therefore changing the composition from 36 to 35 will shift the CET point closer to or further away from the fixed point. The dependence on composition creates a situation with three possible scenarios. The first is when the fixed point is initially located in the columnar region and the CET point moves closer to it. The second is when the fixed point is in the columnar region and the change in

composition makes it cross the CET point and end up in the equiaxed region, which as a result will create a columnar to equiaxed transition that can be observed in the solidified microstructure. The third scenario is when the fixed point is initially located in the equiaxed region and the shifting CET point will move it further into the equiaxed region relative to the original difference. In this case, the equiaxed grain growth conditions are increasingly favoured and the probability of growing smaller nucleation sites into equiaxed grains improves, which in effect can refine an already expected equiaxed microstructure.

3.2. Optical image analysis

The image analysis software ImageJ is used with an algorithm to quickly analyse the microstructure from optical images, the steps of which are presented in figure 4. The process involves changing a 16-bit optical image to an 8-bit greyscale image and thresholding the greyscale values to separate the grains and the grain boundaries. Grains connected to the edge of the image are considered false positives and are removed followed by giving each grain a unique id. The grain size of each identified grain is thereafter exported and analysed or given a colour corresponding to its area to visualise the grain structure.

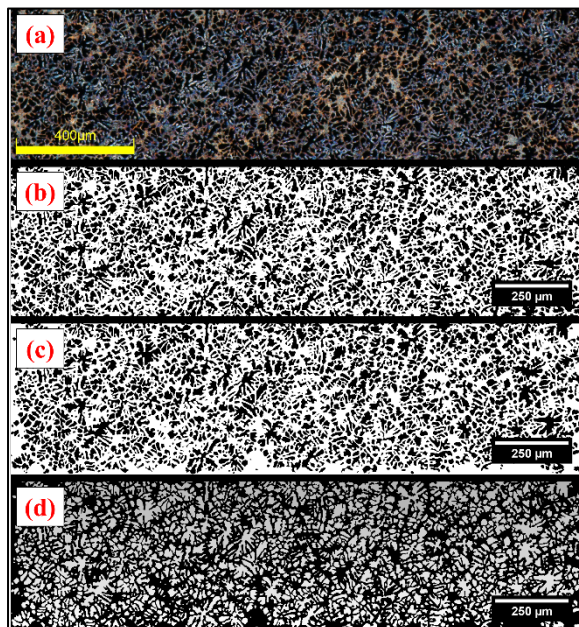


Figure 4. Snapshots from the optical image analysis algorithm. Cropped to the bottom section of a square cross-section. (a) Raw optical image. (b) Thresholded image. (c) Removed edges. (d) Each grain is given an identifying tag.

4. Results and discussion

4.1. Columnar to equiaxed transition

Combining the CET result for each composition at a particular temperature gradient a correlation is found, which can be observed in the plot in figure 5 presenting CET value and silicon concentration. No clear correlation between the other alloying elements is found so the main point of interest is the correlation with the silicon concentration. Increasing the silicon concentration decreases the CET point and can improve the equiaxed grain growth conditions during solidification. However, it is worth to note the rate of change decreases at around 4 wt. % silicon. The red arrows in the figure point to the black spheres which represent the 10 compositions chosen as candidates for further processing with arc melting and experimentally investigated. In addition, the two compositions with 0 wt. % and 0.4 wt. % is also chosen.

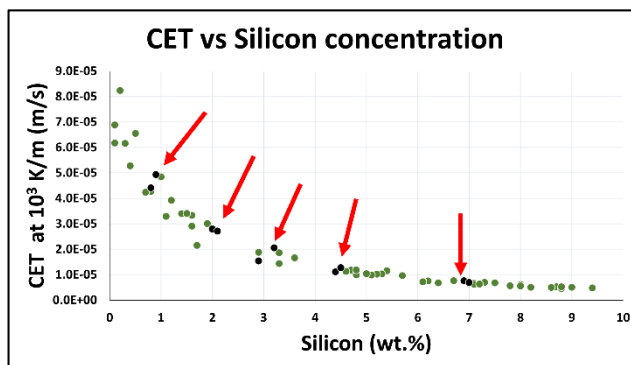


Figure 5. Columnar to equiaxed transition values for each composition plotted against silicon concentration. No correlation is observed with aluminium content but a clear correlation between silicon is evident. The black spheres indicated by the arrows are compositions selected for further experimental investigations.

4.2. Microstructure investigations of compositions with silicon

Applying the optical image analysis algorithm to analyse the microstructure yields an image as presented in figure 6, where the colour of each grain is proportional to its size. The accuracy of the algorithm in measuring the correct grain size is improved by the statistics of analysing many grains at the same time. Therefore, to define a variable representing the material the result of the optical image analysis is chosen to be the average grain size of all grains in the total area. Electron back-scatter diffraction would be an even more accurate method of obtaining the correct size of each grain. However, it is significantly more time consuming and expensive and is not suitable for investigating large quantities of samples which defeats the purpose of rapidly screening material candidates.

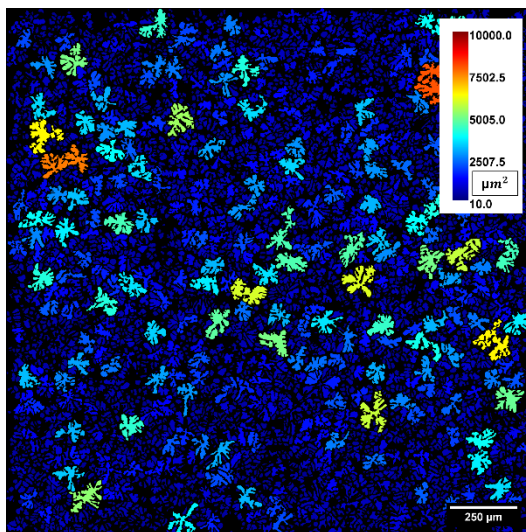


Figure 6: Processed optical image showcasing the result of the optical image analysis algorithm. Each grain is coloured proportional to its size in square microns.

Elemental loss is a common occurrence in both laser powder-bed fusion and arc melting, and energy dispersive spectroscopy is therefore used to find the actual composition of each sample after processing

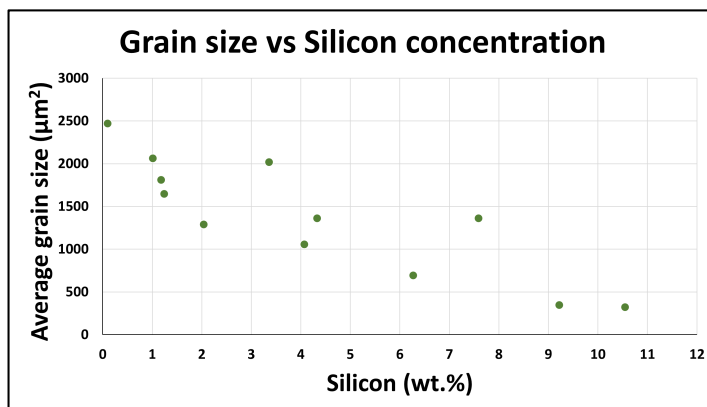


Figure 7. Scatterplot for experimentally obtained grain size to the silicon concentration. A similar trend can be observed in the plot in figure 5, where an increase in silicon concentration reduces the columnar to equiaxed transition point and the average grain size.

has occurred, with a special focus on the silicon concentration. The experimentally obtained composition is presented with the measured average grain size in figure 7. Observing the plot in figure 7 in relation to the plot in figure 5, a clear trend between the silicon concentration in both the thermodynamical calculations and the experimentally obtained grain size is evident. The largest average grain size of $2470 \mu\text{m}^2$ is measured from the composition containing 0 wt.% silicon and the smallest average grain size of $323 \mu\text{m}^2$ comes from the composition containing 10.5 wt.% silicon. In addition to a refinement in grain size, no cracks are observed in the microstructure after the introduction of silicon to the alloy system.

4.1. Microstructure investigations of compositions with silicon and zirconium hydride

The silicon content of the processed sample selected as the candidate to be mixed with zirconium hydride is experimentally measured to 4.68 wt.%. A composition which is located around the point where an increase in silicon concentration does not significantly decrease the CET value at high-temperature gradients. The average grain size for the composition with 4.68 wt.% Si is $1055 \mu\text{m}^2$, which is effectively reduced to $453 \mu\text{m}^2$ and $592 \mu\text{m}^2$ by the inclusion of 0.5 wt.% and 0.8 wt.% zirconium hydride respectively. The addition of zirconium hydride promotes the formation of the Al_3Zr phase, which has the attribute of a low lattice mismatch to the aluminium matrix, and in effect can act as nucleation sites ahead of a moving solidification front. Increasing the number of nucleation sites is another method to promote the formation of more equiaxed grains and in effect refine the microstructure.

5. Conclusion

This work presents a cheap and fast method to rapidly screen a material system to find suitable alloy candidates in an early stage of material development for additive manufacturing. Al-Zn-Mg-Cu alloys blended with different silicon fractions and zirconium hydride were manufactured using arc melting and analysed with optical microscopy and scanning electron microscopy to investigate the effect of silicon and nanoparticles on the microstructure. The main conclusions are drawn as follows:

- Theoretical CET calculations indicate a dependency on silicon concentration. Whereas a higher silicon content reduces the CET point at higher temperature gradients.
- Pressing elemental powder into pellets is shown to be an easy method of creating specific compositions. Arc Melting is shown to be a viable option for quick and inexpensive melting of alloys with similar conditions as present in the laser powder-bed fusion technology.
- The size of each grain in a cross-section of the processed material is obtained from optical images using an image analysis algorithm. The analysis method is shown to be quick and effective in obtaining information about the distribution and approximating the size of each grain.

- The experimentally obtained grain size follows a similar trend to silicon as observed in the theoretical CET calculations, whereas an increased silicon concentration refines the microstructure by reducing the average equiaxed grain size.
- The addition of zirconium is shown to further refine the microstructure compared to the same material without the addition.
- The proposed approach is a cheap, quick and less demanding method for rapid screening of material systems in an early stage of material development for additive manufacturing.

References

- [1] A. Heinz, A. Haszler, C. Keidel, S. Moldenhauer, R. Benedictus and W. Miller, "Recent development in aluminium alloys for aerospace applications," *Materials Science and Engineering: A*, vol. 280, no. 1, pp. 102-107, 2000.
- [2] J. C. Williams and E. A. Starke Jr, "Progress in structural materials for aerospace systems," *Acta materialia*, vol. 51, no. 19, pp. 5775-5799, 2003.
- [3] P. Wang, H. Li, K. Prashanth, J. Eckert and S. Scudino, "Selective laser melting of Al-Zn-Mg-Cu: Heat treatment, microstructure and mechanical properties," *Journal of Alloys and Compounds*, vol. 707, pp. 287-290, 2017.
- [4] L. Li, R. Li, T. Yuan, C. Chen, Z. Zhang and X. Li, "Microstructures and tensile properties of a selective laser melted Al-Zn-Mg-Cu (Al7075) alloy by Si and Zr microalloying," *Materials Science and Engineering: A*, vol. 787, p. 139492, 2020.
- [5] J. Liu, P. Yao, N. Zhao, C. Shi, H. Li, X. Li, D. Xi and S. Yang, "Effect of minor Sc and Zr on recrystallization behavior and mechanical properties of novel Al-Zn-Mg-Cu alloys," *Journal of Alloys and Compounds*, vol. 657, pp. 717-725, 2016.
- [6] V. Zakharov, "Effect of scandium on the structure and properties of aluminum alloys," *Metal science and heat treatment*, vol. 45, no. 7, pp. 246-253, 2003.
- [7] H. Elhadari, H. Patel, D. Chen and W. Kasprzak, "Tensile and fatigue properties of a cast aluminum alloy with Ti, Zr and V additions," *Materials Science and Engineering: A*, vol. 528, no. 28, pp. 8128-8138, 2011.
- [8] M. Gäumann, R. Trivedi and W. Kurz, "Nucleation ahead of the advancing interface in directional solidification," *Materials Science and Engineering: A*, vol. 226, pp. 763-769, 1997.